A $^6A_{1g} \rightarrow {}^4E_g, {}^4A_{1g}$ transition on Mn^{2+} corresponds to a simple spin-flip within the ground state configuration $(t_{2g})^3(e_g)^2$ (O_h notation). We can thus ignore, as we did for the ground state, the orbital part and simply couple the spins.[23] Using the same coupling scheme as for the ground state (see Scheme I), we obtain values shown in Scheme III for the quantum numbers. The range of values for the quantum numbers S_a and S is reduced by one compared to the ground state, and we can schematically draw the splitting pattern shown on the top of Figure 1. In this simplified procedure, we have neglected the effect of excitation transfer. Excitations on the six Mn^{2+} ions are energetically equivalent. They do not represent proper eigenstates of the spin cluster. The proper eigenstates correspond to symmetry-adapted linear combinations of the six locally excited configurations transforming like $A_{1g} + B_{1u} + E_{2g} + E_{1u}$ in the D_{6h} spin-cluster symmetry. Their energies will depend on the magnitude of the excitation transfer integrals between neighboring Mn^{2+} ions.[23] For our present discussion, however, the simplified picture is sufficient. With the selection rules $\Delta S = 0$ and $\Delta S_a = 0, \pm 1$ the two types of transitions I and II shown in Figure 1 are observable, as seen in Figure 7. Band I broadens and shifts to lower energy with increasing temperature as a consequence of populating higher ground-state spin levels. The band at 23 054 cm^{-1} has a temperature dependence corresponding to the Boltzmann population of the $|14,13\rangle$ ground-state level and can thus be assigned to transition II. Its position, 173 cm^{-1} below band I at 1.4 K, can be used to determine the effective J value in the excited state. Within the bilinear approximation, we get

$$2J(^4E_g, {}^4A_{1g}) = -11.6 \text{ cm}^{-1} \quad (7)$$

In Ti^{2+}:$MnCl_2$ the same behavior is observed. The energy difference between bands I and II is 212 cm^{-1}. For the J value in the excited state, we thus get

$$2J(^4E_g, {}^4A_{1g}) = -14.3 \text{ cm}^{-1} \quad (8)$$

Both values are slightly higher than the values of $2J = -10.2$ and -12.4 cm^{-1} obtained by the same approximation for the ground states in Ti^{2+}:$MnBr_2$ and Ti^{2+}:$MnCl_2$, respectively. This is very reasonable when we consider the fact that both the ground and excited state derive from the same strong-field electron configuration on Mn^{2+}. For Mn^{2+}-Mn^{2+} pairs in $CsMgCl_3$ and $CsMgBr_3$, it was found that exchange interactions in the ^4E_g, $^4A_{1g}$ states were about 33% stronger than those in the ground state.[26]

Finally we want to comment on the general appearance of the spin level structure in such a bimetallic cluster; see Figures 3 and 4. It consists of three distinct parts: the degenerate or nearly degenerate ($S_a = S$) levels, a low-energy wing, which may be expanded by biquadratic exchange, consisting of ($S + 1, S$) spin levels and a high-energy wing, which may be compressed by biquadratic exchange, consisting of ($S - 1, S$) levels. Within the low-energy wing the spin level ordering has a ferromagnetic appearance despite the antiferromagnetic nature of the Ti^{2+}-Mn^{2+} exchange. This at first sight paradoxical result arises from the topology and the dominance of Ti^{2+}-Mn^{2+} exchange in our $Ti^{2+}(Mn^{2+})_6$ spin cluster. It can be visualized as shown in Figure 9. $|M_{S_a}, M_S\rangle = |15,14\rangle$ and $|15,16\rangle$ represent the most stable and the least stable configurations of the seven spins for antiferromagnetic Ti^{2+}-Mn^{2+} interaction. The "small" Ti^{2+} spin is thus able to line up all the "large" Mn^{2+} spins in a ferromagnetic-like fashion. This is, of course, the same principle that governs ferrimagnetism in magnetically ordered systems. In this sense the spin cluster studied here can be considered as a ferrimagnetic cluster. With six Mn^{2+} ions surrounding Ti^{2+}, we obtain unusually high spin quantum numbers.

Acknowledgment. We are grateful to Stuart Jacobsen for his help, for many useful discussions, and for providing a crystal. This work was financially supported by the Swiss National Science Foundation and the CNRS of France.

Registry No. $MnCl_2$, 7773-01-5; $MnBr_2$, 13446-03-2; Ti^{2+}, 15969-58-1; Mn^{2+}, 16397-91-4; neutron, 12586-31-1.

(26) McCarthy, P. J.; Güdel, H. U. *Inorg. Chem.* **1984**, *23*, 880.
(27) Furrer, A.; Güdel, H. U. *Phys. Rev. Lett.* **1977**, *39*, 657.

Notes

Contribution from the Department of Chemistry, Monash University, Clayton, Victoria 3168, Australia, and Department of Physical and Inorganic Chemistry, University of Adelaide, Adelaide, South Australia 5001, Australia

Manganese(III) Complexes of a Binucleating Schiff-Base Ligand Based on the 1,3-Diaminopropan-2-ol Backbone

Karen Bertoncello,[1a] Gary D. Fallon,[1a] Keith S. Murray,*[,1a] and Edward R. T. Tiekink[1b]

Received September 12, 1990

As part of our interest in the structural, magnetic,[2,3] and bioinorganic chemical properties[4,5] of manganese complexes, we report here an interesting group of manganese(III) complexes formed with the potentially binucleating ligand 2-OH-SALPN. We had earlier studied binuclear species of this ligand and related ones, with a range of transition-metal ions,[6-9] and our studies of

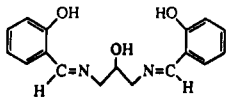

2-OH-SALPN

manganese complexes coincided with a similar study by Pecoraro and Hatfield et al. the results of which have recently been published.[10] Since some of the products were the same, only a brief discussion will be given here of these materials, with emphasis being placed on new aspects not covered by Pecoraro et al.[10] Compounds not obtained by this group will also be highlighted here. In particular, we describe a Na^+-linked polymeric species $[Mn(2\text{-OH-SALPN})(OAc)(NaClO_4)(MeCN)]_x$ (**6**), containing chains of 6-coordinate Mn(III) centers bridged by 7-coordinate Na^+ ions via bridging acetate linkages. This is different in detail

(1) (a) Monash University. (b) University of Adelaide.
(2) Butler, K. D.; Murray, K. S.; West, B. O. *Aust. J. Chem.* **1971**, *24*, 2249.
(3) Kennedy, B. J.; Murray, K. S. *Inorg. Chem.* **1985**, *24*, 1552.
(4) Toftlund, H.; Markiewicz, A.; Murray, K. S. *Acta Chem. Scand.* **1990**, *44*, 443.
(5) Bertoncello, K.; Fallon, G. D.; Murray, K. S. *Inorg. Chim. Acta* **1990**, *174*, 57.
(6) Mazurek, W.; Berry, K. J.; Murray, K. S.; O'Connor, M. J.; Snow, M. R.; Wedd, A. G. *Inorg. Chem.* **1982**, *21*, 3071.
(7) Mazurek, W.; Kennedy, B. J.; Murray, K. S.; O'Connor, M. J.; Rodgers, J. R.; Snow, M. R.; Wedd, A. G.; Zwack, P. R. *Inorg. Chem.* **1985**, *24*, 3258.
(8) Dutton, J. C.; Tiekink, E. R. T.; Murray, K. S. *Inorg. Chim. Acta* **1989**, *166*, 5.
(9) Fallon, G. D.; Markiewicz, A.; Murray, K. S.; Quach, T. *J. Chem. Soc., Chem. Commun.* **1991**, 198.
(10) (a) Bonadies, J. A.; Kirk, M. L.; Lah, M. S.; Kessissoglou, D. P.; Hatfield, W. E.; Pecoraro, V. L. *Inorg. Chem.* **1989**, *28*, 2037. (b) Bonadies, J. A.; Maroney, M. J.; Pecoraro, V. L. *Inorg. Chem.* **1989**, *28*, 2044.

0020-1669/91/1330-3562$02.50/0

from the related trimetallic anionic species $[NaMn_2(2\text{-}OH\text{-}SALPN)_2(OAc)_4]^-$, which contains 6-coordinate Na^+ flanked by two 6-coordinate Mn(III) ions.[10] Coordination of alkali-metal or alkaline-earth-metal cations is also turning out to be a common occurrence in other Mn–chelate systems,[5,11,12] and it is also pertinent to observe that Ca^{2+} ions are important cofactors at the photosynthetic manganese water oxidation center.[13,14]

Separate from the present study and that of Pecoraro et al.[10] are some related ones by Japanese groups in which binuclear dibridged Mn(III) complexes containing the 3-hydroxy-*N,N'*-pentandiylbis(salicylideneamine) backbone and μ-alkoxo or μ-carboxylato exogenous bridges have been described.[15,16] A common observation of all the groups is the weak magnetic exchange coupling between d^4 Mn(III) neighbors that occurs in most such compounds.

Experimental Section

Synthesis. Orange-Colored Precursor (A). A solution of the ligand 2-OH-SALPN[6] (0.745 g, 2.5 mmol) in methanol (20 cm^3) was added to a slurry of manganese(III) acetate dihydrate (1.340 g, 6.25 mmol) in methanol (30 cm^3). The resulting dark brown solution was filtered and sodium perchlorate monohydrate (0.878 g, 6.25 mmol) in methanol (10 cm^3) added to the filtrate. The volume of the solution was reduced to reveal a brown oil. Chloroform (150 cm^3) was added and the mixture refluxed for 30 min, filtered, and reduced to a volume of 50 cm^3 on a rotary evaporator. Addition of petroleum ether gave a fine orange-brown powder (A) (1.585 g). Anal. Calcd for $NaMn_4C_{42}H_{42}N_4O_{18}Cl\cdot 4H_2O$: C, 40.63; H, 4.03; N, 4.51; Cl, 2.86. Found: C, 40.21; H, 4.25; Cl, 3.09. μ_{eff}(291.4 K) = 4.33 μ_B.

Mn^{II}(2-OH-SALPN). The method of Tuchagues et al.[17] was used. The reaction was carried out under an atmosphere of nitrogen, and the yellow product was isolated by using standard Schlenk techniques. Ultraviolet–visible spectrum (MeOH): 216 (26 000 dm^3 mol^{-1} cm^{-1}), 235 (25 900), 290 (15 900), and 692 nm (5440).

[Mn(2-OH-SALPN)(OAc)]$_n$ (1). A solution of (A) (0.100 g) dissolved in acetonitrile (2 cm^3) at room temperature produced tiny green crystals of **1** (0.010 g) within 4 days. Anal. Calcd for $MnC_{19}H_{19}N_2O_5$: C, 55.61; H, 4.63, N, 6.83. Found: C, 55.01; H, 4.86; N, 6.98. Ultraviolet–visible spectrum (MeOH): 224 (31 800 dm^3 mol^{-1} cm^{-1}), 233 (33 500), 271 (20 100), 374 (7630), and 542 nm (296). μ_{eff}(292.3 K) = 4.81 μ_B.

Mn(2-OH-SALPN)(NCS)·1.5H_2O (2·1.5H_2O). A solution of the ligand (0.149 g, 0.5 mmol) in ethanol (5 cm^3) was added to a solution of manganese(II) perchlorate (0.181 g, 0.5 mmol) in ethanol (10 cm^3). Potassium thiocyanate (0.112 g, 1.15 mmol) in ethanol (5 cm^3) was added to the green solution. The potassium perchlorate formed was filtered off and the green solution left to sit at room temperature. The following day, green crystals were isolated (0.115 g, 53%). All physical measurements and analyses were carried out on the crystals obtained straight from the reaction mixture. Anal. Calcd for $MnC_{18}H_{16}N_3O_3S\cdot 1.5H_2O$: C, 49.54; H, 4.36; N, 9.63. Found: C, 49.59; H, 4.42; N, 9.42. Ultraviolet–visible spectrum (MeOH): 213 (35 600 dm^3 mol^{-1} cm^{-1}), 232 (34 800), 274 (19 600), 375 (7200), and 542 nm (314). μ_{eff}(296.0 K) = 4.80 μ_B. X-ray analysis was performed on crystals of the methanolate solvate obtained from a sample recrystallized from methanol.

[Mn_2(2-OH-SALPN)$_2$·THF] (3'). Mn^{II}(2-OH-SALPN) (0.200 g, 0.57 mmol) was gently heated in 200 cm^3 of acetonitrile for 15 min and filtered to remove any undissolved starting material. Oxygen was bubbled through the filtrate for 3 h. Thin green needles were formed by the following day (0.113 g, 57%). These were recrystallized from tetrahydrofuran to give dark brown crystals. Anal. Calcd for $Mn_2C_{34}H_{30}N_4O_6\cdot C_4H_8O$: C, 59.07; H, 4.96; N, 7.25. Found: C, 58.87; H, 4.94; N, 7.02. Ultraviolet–visible spectrum (MeOH): 212 (31 200 dm^3 mol^{-1} cm^{-1} per Mn), 230 (32 200), 271 (19 700), and 373 nm (6980). μ_{eff}(292.0 K) = 4.56 μ_B.

[Mn(2-OH-SALPN)(OAc)($NaClO_4$)(MeCN)]$_x$ (6). A solution of A (1.00 g) dissolved in acetonitrile (15 cm^3) was immediately placed in a refrigerator. Brown crystals of **6** were filtered off after 2 weeks (0.082 g). Anal. Calcd for $NaMnC_{19}H_{19}N_2O_9Cl\cdot CH_3CN$: C, 43.94; H, 3.84; N, 7.32; Cl, 6.18. Found: C, 43.87; H, 4.00; N, 6.99; Cl, 5.85. Ultraviolet–visible spectrum (MeOH): 215 (30 400 dm^3 mol^{-1} cm^{-1}), 234 (33 900), 270 (22 200), and 290 nm (6930). μ_{eff}(292.1 K) = 5.10 μ_B.

Physical Methods. Infrared spectra were measured on a Perkin-Elmer 1600 FT-IR instrument as Nujol mulls. UV–visible spectra were recorded on a Varian Superscan 3 instrument. Chemical analyses were made by the Research School of Chemistry, ANU. Magnetic moments at room temperature were measured by using a Faraday balance incorporating an electromagnet fitted with Faraday profile pole faces.

Magnetic susceptibility data over the range 300–4.2 K were measured on a modified Oxford Instruments Faraday balance. Details have been given previously.[3] A field strength of 10 kOe was used, having first checked for the absence of any field dependent effects at 4.2 K. A nonlinear least-squares fitting program POLYMER (written originally by Dr. F. R. Burden and modified by C. Delfs and Dr. E. N. Bakshi) was used on a VAX 11/780 computer to fit the magnetic data when simple Heisenberg $-2J\vec{S}_1\cdot\vec{S}_2$ models were appropriate. The best-fit criterion was the minimum of the function $R = \sum(\chi_i^{obsd} - \chi_i^{calcd})^2/(\chi_i^{obsd})^2$. Those systems requiring fitting by matrix diagonalization techniques applied to spin Hamiltonians containing zero-field and/or exchange terms required the use of program S2ZFSD (written by K. J. Berry) on a Burroughs 6700 computer, or program MAGB (written by Dr. E. N. Bakshi) on a VAX 11/780 computer.

Collection and Refinement of X-ray Data. Single crystals of **2** were grown from a methanol solution, those of **3'** from tetrahydrofuran and those of **6** from cold acetonitrile. Data were collected on a Philips PW1100 diffractometer (G.D.F. at Monash University) for **2** and **6**, and on an Enraf-Nonius CAD 4F diffractometer (E.R.T.T. at the University of Adelaide) for **3'**. Intensity data were obtained by using graphite-monochromated Mo Kα radiation (0.7107 Å). The data were corrected for Lorentz and polarization effects and for absorption with the use of a numerical procedure[18] (maximum and minimum transmission factors were 0.831 and 0.729 (**2**); 0.861 and 0.693 (**3'**); and 0.959 and 0.930 (**6**), respectively). The atomic scattering factors for neutral atoms were taken from the tables by Hamilton and Ibers[19] or were incorporated in SHELX 76 and were corrected for anomalous dispersion by using values from ref 19. Calculations were performed on a VAX 11/780 (Monash) or a SUN 4/280 (Adelaide) computer. The program used for least-squares refinement was that due to Sheldrick.[18] Table I contains a summary of data collection conditions and results for each of the three structures.

The structures were solved by direct methods[18] and refined by a full-matrix least-squares procedure based on *F*. Anisotropic thermal parameters were used in **2** for Mn, S, and O while isotropic thermal parameters were used for all other non-hydrogen atoms; for **3'**, all non-hydrogen atoms were refined anisotropically; for **6**, anisotropic thermal parameters were used for Mn and the atoms of ClO_4^- while isotropic parameters were used for all other non-hydrogen atoms. In each case hydrogen atoms were included with a single isotropic thermal parameter at their calculated positions (C–H 0.97 Å, except for the OH proton in **6**, which was found from a difference Fourier and included in the refinement as riding on the oxygen). The *R* and *R'* values at convergence are given in Table I where for **2** and **6**, $R' = \sum w^{1/2}(||F_o| - |F_c||)/\sum w^{1/2}|F_o|$) and $w = [\sigma^2(F_o)]^{-1}$ (for **6**) or $[\sigma^2(F_o) + 0.001637(F_o^2)]^{-1}$ (for **2**). The goodness of fit value ($[\sum w(|F_o| - |F_c|^2/(N_{obs} - N_{param})]^{1/2}$) was 1.41 for **2** and 1.73 for **6**. A weighting scheme of the form $2.59[\sigma^2(F) + 0.0005|F|^2]^{-1}$ was used for **3'**. Final atomic coordinates are given in Tables II–IV and the numbering schemes employed are shown in Figures 1–3 all of which were drawn with ORTEP.[20]

Results and Discussion

To aid in discussion we have adopted the same nomenclature and numbering scheme as that used by Pecoraro et al.[10] Close perusal of our synthetic methods and theirs shows significant differences in detail, not the least of which is our use of preformed 2-OH-SALPN ligand compared to their in situ reactions of salicylaldehyde, 1,3-diamino-2-hydroxypropane and Mn(II) or Mn(III) salt. A list of all compounds, including those common to both studies (viz. [Mn(2-OH-SALPN)(OAc)]$_n$ (**1**) and Mn-(2-OH-SALPN)(NCS) (**2**)), together with their magnetic properties, is given in Table V. It should be noted that all

(11) Collins, T. J.; Gordon-Wyllie, S. W. *J. Am. Chem. Soc.* **1989**, *111*, 4511.
(12) Stibrany, R. T.; Gorun, S. M. *Angew. Chem., Int. Ed. Engl.* **1990**, *29*, 1156.
(13) Brudvig, G.; Crabtree, R. H. *Prog. Inorg. Chem.* **1989**, *37*, 99.
(14) Rutherford, A. W. *Trends Biochem. Sci.* **1989**, *14*, 227.
(15) Mikuriya, M.; Kida, S.; Murase, I. *Chem. Lett.* **1988**, 35.
(16) Nishida, Y.; Oshino, N.; Tokii, T. Z. *Naturforsch.* **1988**, *43B*, 472.
(17) Mabad, B.; Cassoux, P.; Tuchagues, J.-P.; Hendrickson, D. N. *Inorg. Chem.* **1986**, *25*, 1420.
(18) Sheldrick, G. M. SHELX 76. Program For Crystal Structure Determination. University of Cambridge, England 1976.
(19) Hamilton, W. C.; Ibers, J. A. *International Tables for X-ray Crystallography*, Kynoch: Birmingham, England, 1974; Vol. IV, pp 99, 149.
(20) Johnson, C. K. ORTEP II. Report ORNL-3794; Oak Ridge National Laboratory: Oak Ridge, TN, 1971.

Table I. Summary of Crystal Data for [Mn(2-OH-SALPN)(NCS)·(MeOH)] (**2**·MeOH), [Mn_2(2-OH-SALPN)$_2$·THF] (**3′**), and [Mn(2-OH-SALPN)(OAc)($NaClO_4$)(MeCN)]$_x$ (**6**)

	2·MeOH	3′	6
formula	$C_{19}H_{20}MnN_3O_4S$	$C_{38}H_{38}Mn_2N_4O_7$	$C_{21}H_{22}MnClN_3NaO_9$
mol wt	441.4	772.6	573.8
space group	$P2_1/n$	$P\bar{1}$	$P2_1/n$
a, Å	12.556 (3)	13.092 (3)	18.744 (4)
b, Å	18.513 (2)	13.410 (4)	11.915 (3)
c, Å	8.796 (1)	9.923 (9)	11.404 (3)
α, deg		93.35 (5)	
β, deg	107.29 (1)	98.62 (5)	103.10 (4)
γ, deg		89.10 (3)	
V, Å^3	1952.2 (6)	1719.5	2480 (1)
Z	4	2	4
d_{calc}, g/cm^3	1.50	1.492	1.54
d_{meas}, g/cm^3	1.50 (1)		1.53 (1)
cryst dimens, mm	0.30 × 0.36 × 0.50	0.50 × 0.50 × 0.22	0.16 × 0.10 × 0.06
radiation	Mo Kα	Mo Kα	Mo Kα
abs coeff, cm^{-1}	7.8	7.29	6.9
scan range, deg	$\pm(0.70 \pm 0.15 \tan\theta)$		$\pm(0.75 + 0.15 \tan\theta)$
bkgd time ratio	0.5	0.5	0.5
2θ, deg	60	45	50
no. of data collcd	5691	4504	4366
no. of data > 3σ(I)	3983	2913	1477
final R	0.051	0.037	0.061
final R'	0.061	0.039	0.053
largest residual, e/Å^3	0.68	0.38	0.48

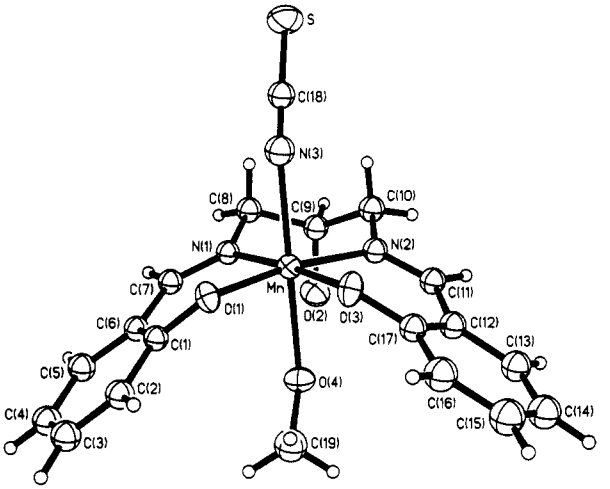

Figure 1. ORTEP diagram of [Mn(2-OH-SALPN)(NCS)·(MeOH)] (**2**·MeOH) showing the atom-numbering scheme.

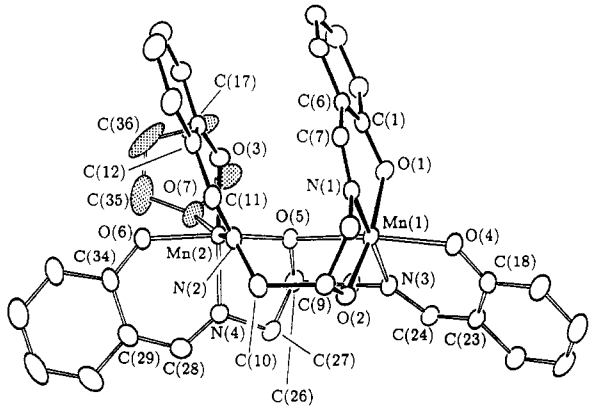

Figure 2. ORTEP diagram of [Mn_2(2-OH-SALPN)$_2$·THF] (**3′**) (showing the atom-numbering scheme) at 25% probability ellipsoids.

compounds except [Mn_2(2-OH-SALPN)$_2$·THF] (**3′**) still retain one of the three protons initially attached to the 2-OH-SALPN ligand.

A key starting material in the synthesis of many of the present compounds was obtained as an orange powder on reacting methanolic solutions of $Mn^{III}(OAc)_3$·$2H_2O$, 2-OH-SALPN, and $NaClO_4$·H_2O, the latter added in anticipation of needing an anion to crystallize desired species of the type [(Mn^{III}_2(2-OH-SALPN)(μ-OAc)(μ-OMe)]$^+$, incorporating only one of the tri-anionic binucleating (2-OH-SALPN)$^{3-}$ ligand groups. While this stoichiometry is common in Cu(II)–Cu(II),[6,7] Ni(II)–Ni(II),[21] VO^{IV}–VO^{IV},[8] and Fe^{III}–Fe^{III}[9] systems it has not been observed in this, or in Pecoraro's study,[10] presumably because of the tendency to achieve 5- or 6-coordination around each Mn(III). The orange-colored intermediate, labeled A, has thus far eluded crystallographic analysis. Its analytical data approximate to the formulation [Mn_2(2-OH-SALPN)(OAc)$_2$]$_2$$NaClO_4$·$4H_2O$.

Table II. Fractional Atomic Coordinates and Thermal Parameters for **2**·MeOH (Esd Values in Parentheses)

atom	x	y	z	U(iso),[a] Å^2
Mn	0.49705 (3)	0.22243 (2)	0.31546 (5)	0.0255 (1)
S	0.3972 (1)	0.1182 (1)	0.7531 (1)	0.0548 (4)
O(1)	0.6498 (2)	0.2076 (1)	0.3410 (3)	0.0314 (7)
O(2)	0.2614 (2)	0.1322 (1)	0.0252 (3)	0.0439 (9)
O(3)	0.5291 (2)	0.3221 (1)	0.3574 (3)	0.0353 (7)
O(4)	0.4738 (2)	0.2419 (1)	0.0492 (2)	0.0360 (7)
C(1)	0.6893 (2)	0.1664 (2)	0.2463 (3)	0.0276 (6)
C(2)	0.7863 (3)	0.1880 (2)	0.2090 (4)	0.0359 (7)
C(3)	0.8300 (3)	0.1460 (2)	0.1138 (4)	0.0397 (7)
C(4)	0.7816 (3)	0.0797 (2)	0.0538 (4)	0.0400 (7)
C(5)	0.6869 (3)	0.0572 (2)	0.0905 (4)	0.0374 (7)
C(6)	0.6373 (2)	0.1012 (2)	0.1809 (3)	0.0297 (6)
C(7)	0.5346 (3)	0.0773 (2)	0.2034 (3)	0.0314 (6)
C(8)	0.3660 (3)	0.0794 (2)	0.2689 (4)	0.0336 (6)
C(9)	0.2607 (3)	0.1210 (2)	0.1841 (4)	0.0351 (6)
C(10)	0.2489 (3)	0.1910 (2)	0.2675 (4)	0.0362 (7)
C(11)	0.2925 (3)	0.3073 (2)	0.2019 (4)	0.0332 (6)
C(12)	0.3569 (3)	0.3702 (2)	0.1907 (4)	0.0329 (6)
C(13)	0.3004 (3)	0.4294 (2)	0.1011 (4)	0.0414 (7)
C(14)	0.3544 (3)	0.4923 (2)	0.0899 (5)	0.0475 (8)
C(15)	0.4684 (4)	0.4979 (2)	0.1728 (5)	0.0521 (9)
C(16)	0.5262 (3)	0.4417 (2)	0.2625 (4)	0.0457 (8)
C(17)	0.4714 (3)	0.3762 (2)	0.2718 (4)	0.0318 (6)
C(18)	0.4586 (3)	0.1615 (2)	0.6411 (4)	0.0338 (6)
C(19)	0.5485 (3)	0.2820 (2)	−0.0147 (5)	0.0490 (9)
N(1)	0.4671 (2)	0.1161 (1)	0.2552 (3)	0.0279 (5)
N(2)	0.3312 (2)	0.2454 (1)	0.2577 (3)	0.0307 (5)
N(3)	0.5005 (2)	0.1928 (2)	0.5602 (4)	0.0401 (6)

[a] The equivalent isotropic temperature factor for Mn, S, and O is defined as one-third of the orthogonalized U tensor.

(21) Mazurek, W.; Bond, A. M.; O'Connor, M. J.; Wedd, A. G. *Inorg. Chem.* **1986**, *25*, 906.

Table III. Fractional Atomic Coordinates ($\times 10^5$ for Mn; $\times 10^4$ for Other Atoms) for **3'**

atom	x	y	z
Mn(1)	9531 (5)	-25297 (5)	-10621 (6)
Mn(2)	36527 (4)	-26900 (5)	8329 (6)
O(1)	284 (2)	-2496 (2)	511 (3)
O(2)	1787 (2)	-2444 (2)	-2419 (3)
O(3)	3258 (2)	-1839 (2)	2231 (3)
O(4)	-429 (2)	-2309 (2)	-2370 (3)
O(5)	2333 (2)	-3258 (2)	356 (3)
O(6)	5070 (2)	-2405 (2)	1379 (3)
O(7)	3912 (3)	-3930 (3)	2713 (3)
N(1)	1229 (2)	-1086 (2)	-754 (3)
N(2)	3508 (2)	-1369 (3)	-470 (3)
N(3)	727 (3)	-4033 (3)	-1511 (3)
N(4)	4018 (3)	-3695 (3)	-582 (3)
C(1)	487 (3)	-1881 (3)	1610 (4)
C(2)	272 (3)	-2167 (4)	2866 (5)
C(3)	451 (4)	-1543 (4)	4027 (5)
C(4)	838 (4)	-588 (4)	3962 (5)
C(5)	1038 (3)	-280 (3)	2745 (4)
C(6)	879 (3)	-908 (3)	1556 (4)
C(7)	1174 (3)	-542 (3)	346 (4)
C(8)	1537 (3)	-690 (3)	-1985 (4)
C(9)	2203 (3)	-1500 (3)	-2578 (4)
C(10)	3350 (3)	-1423 (4)	-1960 (4)
C(11)	3714 (3)	-515 (3)	135 (5)
C(12)	3781 (3)	-251 (3)	1576 (5)
C(13)	4011 (4)	751 (4)	2010 (6)
C(14)	4035 (4)	1089 (4)	3341 (6)
C(15)	3816 (4)	435 (4)	4282 (6)
C(16)	3584 (3)	-530 (3)	3892 (5)
C(17)	3543 (3)	-906 (3)	2546 (4)
C(18)	-879 (3)	-2899 (4)	-3351 (4)
C(19)	-1673 (4)	-2522 (4)	-4325 (5)
C(20)	-2169 (4)	-3137 (5)	-5364 (6)
C(21)	-1908 (4)	-4135 (5)	-5504 (5)
C(22)	-1167 (4)	-4531 (4)	-4574 (5)
C(23)	-626 (3)	-3933 (4)	-3482 (4)
C(24)	110 (3)	-4430 (3)	-2520 (5)
C(25)	1344 (4)	-4692 (4)	-580 (5)
C(26)	2420 (3)	-4283 (3)	-113 (5)
C(27)	3126 (4)	-4312 (3)	-1182 (5)
C(28)	4908 (3)	-3806 (3)	-988 (4)
C(29)	5809 (3)	-3248 (3)	-457 (5)
C(30)	6700 (4)	-3367 (4)	-1104 (6)
C(31)	7600 (4)	-2890 (5)	-594 (7)
C(32)	7646 (4)	-2291 (5)	596 (7)
C(33)	6805 (3)	-2138 (4)	1230 (5)
C(34)	5865 (3)	-2588 (3)	722 (4)
C(35)	4776 (6)	-3759 (7)	3741 (8)
C(36)	4407 (10)	-3356 (7)	4942 (10)
C(37)	3320 (9)	-3495 (6)	4770 (7)
C(38)	3027 (5)	-3982 (5)	3410 (6)

Compound A presumably contains the structural ingredients of, or precursor to, **6** since dissolution in ice-cold MeCN yields brown crystals of the Na^+-coordinated polymeric material **6** (vide infra) while dissolution in MeCN at ambient temperature produces green crystals of the linear-chain μ-acetato(anti-syn)-bridged complex $[Mn(2\text{-OH-SALPN})(OAc)]_n$ (**1**).[10]

Mn(2-OH-SALPN)NCS·1.5H$_2$O (2·1.5H$_2$O). Crystals grown from methanol show the six-coordinate structure displayed in Figure 1 in which N-bonded NCS and methanol occupy the axial sites. Bond distances and angles are given in Table VI. The methanol ligand lies under the "umbrella" of the 2-OH-SALPN moiety at a Mn–O(4) distance of 2.301 (2) Å. It is likely that water occupies this position in the parent complex, **2**·1.5H$_2$O.

Magnetic studies on **2**·1.5H$_2$O show that μ_{eff} decreases from 4.80 μ_B at 295 K to 3.17 μ_B at 4.2 K in a manner characteristic of a zero-field split ^{5}A ground-state.[3] Spin-Hamiltonian ($S = 2$) analysis of the data using a $D\tilde{S}_z^2$ Hamiltonian gave a best-fit $|D|$ value of 12 cm^{-1}. However, comparison to the $|D|$ values of related complexes such as Mn(salen)(NCS) ($D = -3.8$ cm^{-1}),[3] would suggest that this value of $|D|$ is overestimated and that weak antiferromagnetic exchange coupling may also be occurring. Careful perusal of the χ/T or χ^{-1}/T plot near to 4.2 K (Figure 4) shows that the χ values are leveling off and may go through a maximum at T less than 4.2 K compatible with a J value of ca. -0.3 cm^{-1} and a D value of ca. 4 cm^{-1}. Field-dependent magnetization studies at very low temperatures are required to confirm the presence of exchange effects. Inspection of the crystal packing diagram of the methanol adduct of **2** shows that there are no obvious Mn···Mn interactions; however, it is possible that appropriate pathways do exist in the parent hydrated complex.

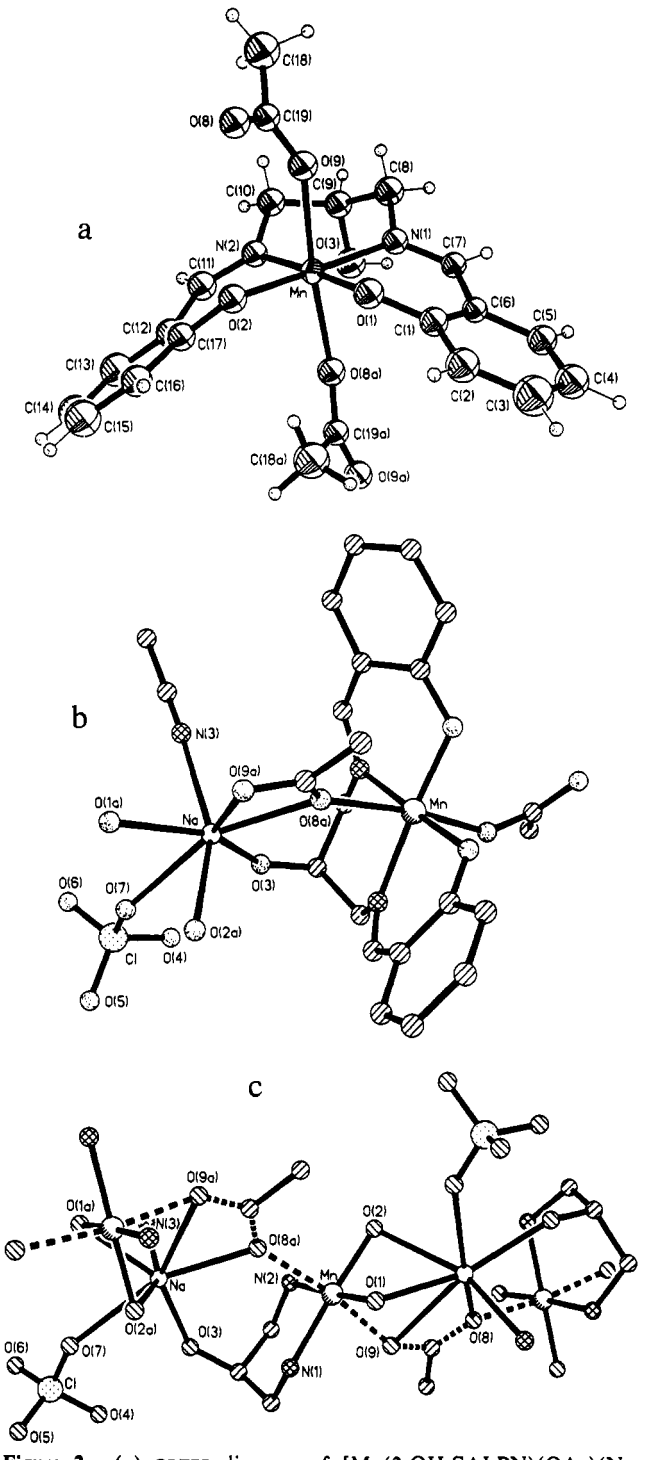

Figure 3. (a) ORTEP diagram of [Mn(2-OH-SALPN)(OAc)(Na-ClO$_4$)(MeCN)]$_x$ (**6**) showing the atom-numbering scheme. The six-coordinate geometry around each Mn center is displayed. (b) Diagram showing the Na and Mn coordination environments in **6**. (Note that O(1a) is equivalent to O(1)* in Table VIII). (c) Simplified diagram showing the acetato-bridged polymeric structure (dotted line) in **6**.

[Mn$_2$(2-OH-SALPN)$_2$·THF] (3'). This complex was obtained by reacting Mn^{II}(2-OH-SALPN) with O_2 in acetonitrile. The reaction was initially done to see if a (μ-dioxo)manganese(IV)

Table IV. Fractional Atomic Coordinates and Thermal Parameters for **6** (Esd Values in Parentheses)

atom	*x*	*y*	*z*	*U*(Iso), Å^2
Mn	0.7670 (1)	0.1954 (1)	0.2362 (1)	*a*
Cl	0.9185 (2)	−0.2379 (3)	−0.0596 (3)	*a*
O(4)	0.9439 (4)	−0.1232 (7)	−0.0630 (8)	*a*
O(5)	0.9767 (5)	−0.3074 (9)	−0.0044 (11)	*a*
O(6)	0.8896 (7)	−0.2769 (8)	−0.1767 (8)	*a*
O(7)	0.8632 (5)	−0.2398 (7)	0.0052 (9)	*a*
Na	0.7695 (2)	−0.1169 (4)	0.0892 (4)	0.041 (1)
C(1)	0.8128 (5)	0.1175 (9)	0.4790 (10)	0.030 (3)
C(2)	0.7937 (6)	0.1058 (9)	0.5915 (10)	0.039 (3)
C(3)	0.8282 (7)	0.0227 (10)	0.6692 (12)	0.054 (4)
C(4)	0.8812 (6)	−0.0460 (10)	0.6424 (10)	0.041 (3)
C(5)	0.9006 (6)	−0.0342 (9)	0.5361 (10)	0.032 (3)
C(6)	0.8673 (5)	0.0479 (8)	0.4515 (9)	0.024 (3)
C(7)	0.8954 (6)	0.0640 (8)	0.3462 (9)	0.026 (3)
C(8)	0.9109 (6)	0.1469 (10)	0.1651 (10)	0.038 (3)
C(9)	0.8715 (6)	0.1254 (9)	0.0366 (10)	0.034 (3)
C(10)	0.8077 (5)	0.2045 (10)	−0.0095 (9)	0.034 (3)
C(11)	0.6811 (5)	0.1869 (9)	−0.0096 (10)	0.036 (3)
C(12)	0.6157 (6)	0.1932 (9)	0.0335 (9)	0.032 (3)
C(13)	0.5483 (6)	0.1722 (9)	−0.0458 (11)	0.047 (3)
C(14)	0.4827 (6)	0.1915 (10)	−0.0136 (11)	0.047 (3)
C(15)	0.4826 (7)	0.2365 (9)	0.0944 (11)	0.048 (3)
C(16)	0.5468 (6)	0.2616 (8)	0.1784 (10)	0.035 (3)
C(17)	0.6142 (6)	0.2403 (8)	0.1486 (10)	0.029 (3)
C(18)	0.8646 (6)	0.5144 (10)	0.1610 (11)	0.048 (4)
C(19)	0.8167 (6)	0.4602 (9)	0.2317 (9)	0.026 (3)
C(20)	0.5985 (8)	−0.0589 (14)	−0.3149 (14)	0.098 (6)
C(21)	0.6482 (7)	−0.0709 (11)	−0.1982 (14)	0.062 (4)
N(1)	0.8671 (4)	0.1247 (7)	0.2548 (8)	0.028 (2)
N(2)	0.7470 (4)	0.1924 (7)	0.0547 (7)	0.029 (2)
N(3)	0.6845 (6)	−0.0828 (9)	−0.1093 (11)	0.072 (4)
O(1)	0.7803 (3)	0.1974 (6)	0.4053 (6)	0.033 (2)
O(2)	0.6760 (3)	0.2664 (5)	0.2265 (6)	0.030 (2)
O(3)	0.8464 (4)	0.0122 (6)	0.0202 (7)	0.043 (2)
H(O3)	0.8653 (4)	−0.0219 (6)	0.0823 (7)	0.073 (8)
O(8)	0.7758 (4)	0.5176 (6)	0.2790 (6)	0.032 (2)
O(9)	0.8218 (3)	0.3547 (6)	0.2415 (6)	0.033 (2)

[a] See supplementary material for anisotropic thermal parameters.

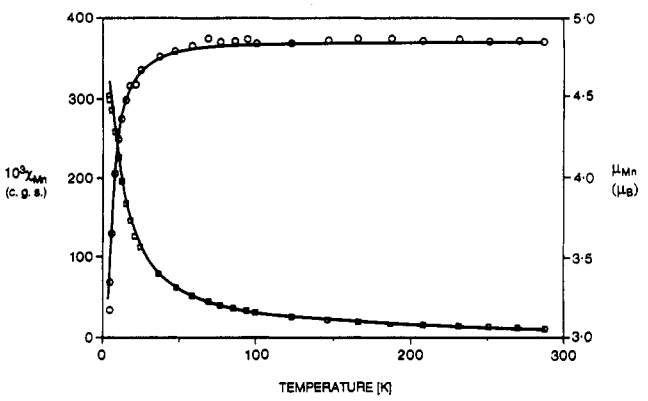

Figure 4. Magnetic susceptibility (□) and moment data (○) for **2**·1.5H_2O. The solid line is that calculated by using fit 1 parameters (Table V). Similar calculated values were given for fit 2.

compound of the type obtained with the SALPN ligand, viz. $[Mn^{IV}(SALPN)O]_2$[22-25] or some other oxygenated species, could be obtained. However, oxidation cases at the Mn^{III} level in the present case.

Crystallization from THF of the product obtained from MeCN yielded crystals suitable for X-ray diffraction studies. Pecoraro et al.[10] were not able to obtain X-ray quality crystals of the analogous methanol solvate $[Mn_2(2\text{-OH-SALPN})_2(MeOH)]$·MeOH (**3**) and so used the 5-Cl-SALPN analogue **4** for crystallography. Interestingly these workers required that stoichiometric equivalents of base be added to aerobically stirred solutions of Mn(II) salt, salicylaldehyde, and 1,3-diamino-2-hydroxypropane or to $[Mn(2\text{-OH-SALPN})]^+$ solutions in order to produce the binuclear species. Clearly this was not required here.

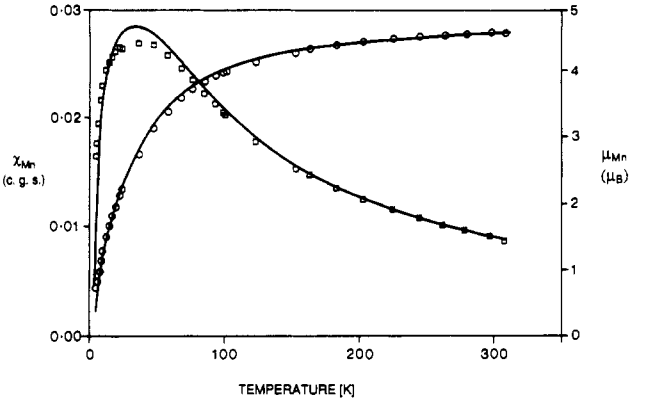

Figure 5. Magnetic susceptibility (□) and moment (○) data for **3′**. The solid line is that calculated by using the parameters given in Table V and in the text.

The crystal structure of **3′** shows the same novel binuclear structure as in **4** except for the THF molecule, which occupies the MeOH site. Selected bond lengths and angles for **3′** are listed in Table VII. In the binuclear compound, there are two distorted octahedral geometries about the Mn atoms by virtue of the presence of two distinct trinegative, pentadentate 2-OH-SALPN ligands and a coordinated THF molecule see Figure 2. One ligand bridges both Mn centers via an alkoxide bridge, O(5), and chelates each Mn atom via the imino phenolate portions of its donor set. The second ligand coordinates Mn(1) via the alkoxide atom, O(2), and the N(1) and O(1) atoms and at the same time coordinates Mn(2) via the N(2) and O(3) atoms. The sixth coordination site for Mn(2) is occupied by the O(7) atom of the THF molecule.

The alkoxide bridge is not symmetrical, forming a shorter bond to Mn(2) of 1.883 (3) Å (cf. Mn(1)–O(5) = 2.353 (3) Å); the Mn(1)–O(5)–Mn(2) angle is 124.5 (1)°. The Mn(1)···Mn(2) separation is 3.756 (2) Å. All of the metrical details are somewhat similar in the case of **4**, except that the Mn(1)···Mn(2) separation is longer (3.808 (1) Å) and the Mn(1)–O(5)–Mn(2) bridge angle is correspondingly larger (128.9 (2)°).[10]

The temperature variation of the magnetic susceptibilities of **3′**, shown in Figure 5, is typical of an antiferromagnetically coupled $S_1 = 2$ and $S_2 = 2$ dimer, with a χ_{max} value at 35 K. Least-squares fitting to a simple symmetrical $-2J\hat{S}_1\cdot\hat{S}_2$ model gave a good fit for $g_1 = g_2 = 2.00$ and $J = -5.5$ cm^{-1}. This J value is larger than it is in **4** (i.e. −3.55 cm^{-1}) probably because of a combination of the small differences in bridge geometry mentioned above and of the different substituents (5-Cl vs 5-H), on the salicylaldehyde ring. These negative J values are greater in size than those obtained for the bis(μ-phenolato) 90° bridges found[3] in $[Mn(SALEN)Cl]_2$ but much less than that recently obtained[25] for another corner-shared example, the μ-oxo Schiff-base complex $Mn_2O(5\text{-}NO_2\text{-SALDIEN})_2$ ($J = -120$ cm^{-1}, Mn–O–Mn = 168.4 (2)°, Mn–O = 1.74 Å, Mn···Mn = 3.490 (2) Å). As pointed out by Pecoraro and Hatfield et al.,[10] superexchange at the bridging alkoxo O atom in **3′** and **4** formally involves the d_{z^2} orbital on Mn(1) and the $d_{x^2-y^2}$ orbital (unoccupied) on Mn(2), a situation expected to lead to very weak coupling. In contrast, the magnetic orbitals, which point towards the oxo bridge in $Mn_2O(5\text{-}NO_2\text{-SALDIEN})_2$, are both likely to be $d_{x^2-y^2}$ (where z is defined along the long axial bonds) but are oriented at ca. 90° to each other, since the equatorial planes around each Mn are not coplanar. These orbitals are both unoccupied. Armstrong et al.[25] have speculated that this unusual orbital orientation effect may, in part, influence the size of J.

Comparison of the data for **3′** and **4** with that for the μ-oxo complex suggests that the bridging {Mn–X–Mn} bond distances

(22) Boucher, L. J.; Coe, C. G. *Inorg. Chem.* **1975**, *14*, 1289.
(23) Gohdes, J. W.; Armstrong, W. H. Unpublished results.
(24) Li, X.; Larson, E.; Bonadies, J.; Lah, M. S.; Pecoraro, V. L. Unpublished data.
(25) Kipke, C. A.; Scott, M. J.; Gohdes, J. W.; Armstrong, W. H. *Inorg. Chem.* **1990**, *29*, 2193.

Table V. Magnetic Properties of Manganese(III)-2-OH-SALPN Complexes[a]

complex	μ_{eff}/Mn (μ_B)	J, cm^{-1}	$\lvert D\rvert$, cm^{-1}	color	ref
Mn(2-OH-SALPN)(OAc)$_n$ (**1**)	4.85	−1.72	nd	green	10
Mn(2-OH-SALPN)(NCS) (**2**)	5.02	nd	nd	green	10
Mn(2-OH-SALPN)(NCS)·1.5H$_2$O (**2**·1.5H$_2$O)	4.80	0[b]	12	green	tw
		−0.3[c]	4		
[Mn$_2$(2-OH-SALPN)$_2$(MeOH)]·MeOH (**3**)	4.76	nd	nd	green/brown	10
[Mn$_2$(2-OH-SALPN)$_2$·THF] (**3′**)	4.56	−5.5	nd	brown	tw
[Mn$_2$(2-OH[5-Cl-SAL]PN)$_2$(MeOH)]·MeOH (**4**)	4.85	−3.55	nd	green/brown	10
[C$_2$H$_9$O$_2$][NaMn$_2$(2-OH-SALPN)$_2$(OAc)$_4$]·2H$_2$O (**5**)	5.01	0	6.13	green	10
[Mn(2-OH-SALPN)(OAc)(NaClO$_4$)(MeCN)]$_x$ (**6**)	5.10	−0.5	2	brown	tw

[a] Key: nd = not determined; tw = this work. [b] Fit 1. [c] Fit 2.

Table VI. Selected Bond Distances (Å) and Angles (deg) for **2**

Mn–O(1)	1.882 (2)	Mn–N(3)	2.210 (3)
Mn–O(3)	1.902 (2)	Mn–O(4)	2.301 (2)
Mn–N(2)	2.036 (3)	S–C(18)	1.630 (4)
Mn–N(1)	2.044 (3)	N(3)–C(18)	1.158 (5)
O(1)–Mn–O(3)	88.3 (1)	N(2)–Mn–N(1)	92.3 (1)
O(1)–Mn–N(2)	171.8 (1)	N(2)–Mn–N(3)	91.0 (1)
O(1)–Mn–N(1)	89.6 (1)	N(2)–Mn–O(4)	84.4 (1)
O(1)–Mn–N(3)	97.1 (1)	N(1)–Mn–N(3)	87.8 (1)
O(1)–Mn–O(4)	87.8 (1)	N(1)–Mn–O(4)	85.9 (1)
O(3)–Mn–N(2)	89.3 (1)	N(3)–Mn–O(4)	172.1 (1)
O(3)–Mn–N(1)	175.5 (1)	N(3)–C(18)–S	178.8 (3)
O(3)–Mn–N(3)	96.3 (1)	C(18)–N(3)–Mn	147.4 (2)
O(3)–Mn–O(4)	90.1 (1)	C(19)–O(4)–Mn	125.4 (2)

Table VII. Selected Bond Distances (Å) and Angles (deg) for **3′**

Mn(1)–O(1)	1.899 (3)	Mn(2)–O(3)	1.871 (3)
Mn(1)–O(2)	1.866 (3)	Mn(2)–O(5)	1.883 (3)
Mn(1)–O(4)	2.091 (3)	Mn(2)–O(6)	1.892 (3)
Mn(1)–O(5)	2.353 (3)	Mn(2)–O(7)	2.552 (3)
Mn(1)–N(1)	1.973 (3)	Mn(2)–N(2)	2.243 (3)
Mn(1)–N(3)	2.055 (3)	Mn(2)–N(4)	1.994 (3)
Mn(1)···Mn(2)	3.756 (2)		
O(1)–Mn(4)–O(2)	170.4 (1)	O(3)–Mn(2)–O(5)	93.9 (1)
O(1)–Mn(1)–O(4)	92.9 (1)	O(3)–Mn(2)–O(6)	92.5 (1)
O(1)–Mn(1)–O(5)	84.5 (1)	O(3)–Mn(2)–O(7)	82.6 (1)
O(1)–Mn(1)–N(1)	90.0 (1)	O(3)–Mn(2)–N(2)	87.4 (1)
O(1)–Mn(1)–N(3)	94.5 (1)	O(3)–Mn(2)–N(4)	174.9 (1)
O(2)–Mn(1)–O(4)	94.6 (1)	O(5)–Mn(2)–O(6)	167.7 (1)
O(2)–Mn(1)–O(5)	90.0 (1)	O(5)–Mn(2)–O(7)	85.4 (1)
O(2)–Mn(1)–N(1)	83.6 (1)	O(5)–Mn(2)–N(2)	101.1 (1)
O(2)–Mn(1)–N(3)	92.0 (1)	O(5)–Mn(2)–N(4)	82.9 (1)
O(4)–Mn(1)–O(5)	163.3 (1)	O(6)–Mn(2)–O(7)	85.0 (1)
O(4)–Mn(1)–N(1)	93.3 (1)	O(6)–Mn(2)–N(2)	89.7 (1)
O(4)–Mn(1)–N(3)	86.7 (1)	O(6)–Mn(2)–N(4)	90.0 (1)
O(5)–Mn(1)–N(1)	103.2 (1)	O(7)–Mn(2)–N(2)	168.4 (1)
O(5)–Mn(1)–N(3)	77.1 (1)	O(7)–Mn(2)–N(4)	93.2 (1)
N(1)–Mn(1)–N(3)	175.5 (1)	N(2)–Mn(2)–N(4)	97.0 (1)
Mn(1)–O(5)–Mn(2)	124.5 (1)		

and angles, perhaps allied with superexchange pathways involving out-of-plane (π-type) Mn orbitals with the appropriate orbital on X = O^{2-} or OR^-, will all play a part. It is interesting also to note that the recent model of Wieghardt and Girerd et al.,[26] which invokes the lack of "cross" pathways of the type d_{z^2}–d_{xz} to explain weak antiferromagnetism or ferromagnetism in triply bridged (μ-oxo)bis(μ-carboxylato)dimanganese(III) complexes (where z is now defined as the short Mn–O(oxo bridge) direction), cannot readily explain the strong antiferromagnetism in $Mn_2O(5\text{-}NO_2\text{-}SALDIEN)_2$.

[Mn(2-OH-SALPN)(OAc)(NaClO$_4$)(MeCN)]$_x$ (6). The crystal structure of this unusual polymeric species shows some interesting facets. Each six-coordinate [Mn(2-OH-SALPN)(OAc)]$_x$ moiety is very similar in ligand conformation, and coordination geometry around Mn, to those in [Mn(2-OH-SALPN)(OAc)]$_n$[10] and [Mn(2-OH-SALPN)(NCS)(MeOH)]—see Figure 3a. The polymeric acetato-bridged manganese(III) zigzag chain structure is simplified in Figure 3b,c. The acetate bridges are in anti–syn orientation and the Mn–O intrachain distances are unsymmetrical, e.g. Mn–O (9) = 2.152 (7) and Mn–O (8a) = 2.258 (7) Å, and significantly longer than the in-plane Mn–O distances (1.887 (7) Å). Encapsulated between each Mn···Mn pair is a seven-coordinate Na$^+$ ion. As is evident from Table VIII the Na$^+$ ions show contact distances of ca. 2.5 Å to the O(8) and O(9) atoms from the bridging acetate, the O(3) atom from the (uncoordinated) alcohol, the O(1) and O(2) phenolate atoms of (2-OH-SALPN)Mn, the O(7) of ClO_4^-, and the N(3) of MeCN. These structural features are quite different from those observed[10] in [NaMn$_2$(2-OH-SALPN)$_2$(OAc)$_4$]$^-$ (**5**) in which Mn···Mn pairs are not bridged directly by acetate groups but by an encapsulated Na$^+$ ion, which, in turn, is bridged to each Mn via an acetate and the two *cis*-phenolate oxygen atoms from the (2-OH-SALPN)Mn moiety. The alcohol oxygen atom is not coordinated to Na$^+$ in **5**.

Table VIII. Selected Bond Distances (Å) and Angles (deg) for **6**[a]

Mn–O(1)	1.877 (7)	Na–O(3)	2.36 (1)
Mn–O(2)	1.885 (7)	Na–O(7)	2.63 (1)
Mn–N(1)	2.023 (9)	Na–O(1)*	2.41 (1)
Mn–N(2)	2.018 (8)	Na–O(2)*	2.53 (1)
Mn–O(9)	2.152 (7)	Na–O(8)*	2.48 (1)
Mn–O(8)*	2.258 (7)	Na–O(9)*	2.87 (1)
Na–N(3)	2.49 (1)		
O(1)–Mn–O(2)	87.8 (3)	O(3)–Na–N(3)	84.5 (4)
O(1)–Mn–N(1)	89.7 (3)	O(3)–Na–O(2)*	118.2 (3)
O(1)–Mn–N(2)	176.9 (3)	O(3)–Na–O(7)	74.5 (3)
O(1)–Mn–O(9)	90.5 (3)	O(3)–Na–O(9)*	143.2 (3)
O(1)–Mn–O(8)*	93.0 (3)	O(1)*–Na–O(18)*	113.0 (3)
O(2)–Mn–N(1)	176.8 (3)	O(1)*–Na–N(3)	90.1 (3)
O(2)–Mn–N(2)	89.6 (3)	O(1)*–Na–O(2)*	63.9 (2)
O(2)–Mn–O(9)	91.4 (3)	O(1)*–Na–O(7)	78.0 (3)
O(2)–Mn–O(8)*	96.7 (3)	O(1)*–Na–O(9)*	65.2 (2)
N(1)–Mn–N(2)	93.0 (4)	O(8)*–Na–N(3)	102.1 (3)
N(1)–Mn–O(9)	86.5 (3)	O(8)*–Na–O(2)*	88.9 (3)
N(1)–Mn–O(8)*	85.5 (3)	O(8)*–Na–O(7)	158.7 (3)
N(2)–Mn–O(9)	91.2 (3)	O(8)*–Na–O(9)*	47.9 (2)
N(2)–Mn–O(8)*	85.7 (3)	N(3)–Na–O(2)*	154.0 (3)
O(9)–Mn–O(8)*	171.3 (3)	N(3)–Na–O(7)	95.9 (4)
Mn–O(9)–C(19)	148.1 (7)	N(3)–Na–O(9)*	105.9 (4)
C(19)*–O(8)*–Mn	136.8 (7)	O(2)*–Na–O(7)	79.6 (3)
O(3)–Na–O(1)*	151.3 (3)	O(2)*–Na–O(9)*	64.4 (2)
O(3)–Na–O(8)*	95.7 (3)	O(7)–Na–O(9)*	136.7 (3)

[a] An asterisk denotes an atom transformed through symmetry element $1.5 - x, y - 0.5, 0.5 - z$.

These structural differences between **5** and **6** are reflected in their magnetic properties. Hatfield and co-workers[10] obtained a D value of −6.1 cm^{-1} for **5** by using a spin-Hamiltonian analysis, the lack of any exchange coupling (i.e. $J = 0$) being due to the absence of any Mn(μ-OAc)Mn bridging pathway. The μ_{Mn} values for **6** decreased a little from 5.08 μ_B at 295 K to 4.8 μ_B at 60 K and then decreased more rapidly to reach 3.17 μ_B at 4.2 K. The corresponding χ_{Mn}/T plot did not show any maximum above 4.2 K, but the unrealistically high $\lvert D\rvert$ value of 20 cm^{-1} obtained by a ZFS analysis of the data strongly suggested that weak antiferromagnetic coupling was occurring via the bridging acetate

(26) Bossek, U.; Weyhermüller, T.; Wieghardt, K.; Bonvoisin, J.; Girerd, J. J. *J. Chem. Soc. Chem. Commun.* **1989**, 633.

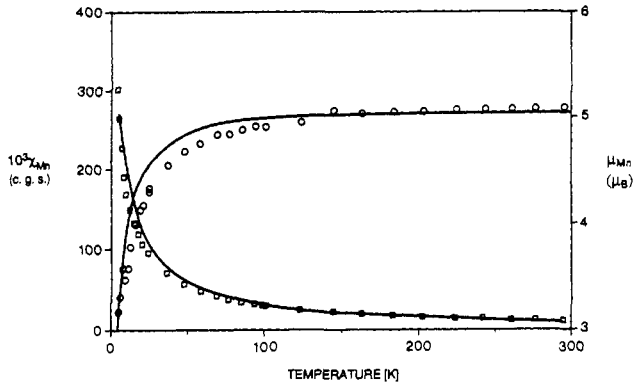

Figure 6. Magnetic susceptibility (□) and moment (○) data for **6**. The solid line is that calculated by using the parameters given in Table V and in the text.

network. A reasonably good fit of the data, shown in Figure 6, was achieved by using matrix diagonalization techniques for a Hamiltonian appropriate to $S = 2$ pairs which included $D\tilde{S}_z^2$, $-2J\tilde{S}_1 \cdot \tilde{S}_2$, and Zeeman terms,[3] the best-fit parameters being $g = 2.08$, $J = -0.5$ cm^{-1}, and $|D| = 2$ cm^{-1}, the latter presumably being negative in sign in view of the axially elongated structure around Mn(III). The moderate agreement between observed and calculated values in the region 10-30 K probably is due to lack of inclusion of a rhombic (E) ZFS term or to the binuclear approximation employed.

Conclusions

The rich series of manganese(III) Schiff-base structures described here complements and extends that recently described by Pecoraro et al.[10] Use of the 2-OH-SALPN ligand, in conjunction with carboxylate or other anionic ligands, and alkali-metal ions can lead to the formation of mono-, bi-, or polynuclear Mn(III) complexes. The particular role of the Na^+ ion in **5** and **6** is a subtle one and has been emphasized by Pecoraro et al.[10] in relation to the cofactor role that alkali-metal or alkaline-earth-metal ions are known to play in the manganese site of the photosystem II water oxidation center.

As in other recent studies, we have shown that Mn(III)···Mn(III) exchange interactions in these and other related systems are weakly antiferromagnetic in origin and modulated by zero-field splitting effects. We have attempted to briefly summarize, where appropriate, the current state of Mn(III) magnetostructural correlations and find that while it is possible to generally understand the weak net coupling, interpretation of small differences in J largely depends on the relative orientations of the elongated (or compressed) axial directions on each $S = 2$ Mn(III) center. To date, the strongest coupling has been observed in μ-oxo singly bridged Mn(III)-O-Mn(III)[25] or in doubly bridged $Mn^{III}_2(O)_2$ systems.[27]

Acknowledgment. Dr. A. Markiewicz and Mr. K. J. Berry are thanked for their help with the magnetic work. This work was supported by grants from the Australian Research Council and Monash University Research Grants.

Registry No. **1**, 120205-66-5; **2**·$^3/_2H_2O$, 135366-41-5; **2**·MeOH, 135366-43-7; **3'**, 135366-42-6; **6**, 135366-45-9; Mn(2-OH-SALPN), 69879-57-8.

Supplementary Material Available: For complex **3'**, Table S1 (fractional coordinates and anisotropic thermal parameters for non-hydrogen atoms), Table S2 (hydrogen atom parameters and anisotropic thermal parameters), Table S3 (bond distances), and Table S4 (bond angles), for complex **2**·MeOH, Table S6 (hydrogen atom parameters and anisotropic thermal parameters), Table S7 (bond distances), and Table S8 (bond angles), and for complex **6**, Table S10 (hydrogen atom parameters), Table S11 (bond distances), and Table S12 (bond angles) (14 pages); for all three complexes, Tables S5, S9, and S13 (structure factors) (34 pages). Ordering information is given on any current masthead page.

(27) Goodson, P. A.; Oki, A. R.; Glerup, J.; Hodgson, D. J. *J. Am. Chem. Soc.* **1990**, *112*, 6248.

Contribution from the Laboratory for Inorganic Chemistry, ETH-Zentrum, CH-8092 Zurich, Switzerland, and Istituto di Chimica Farmaceutica, University of Milan, I-20131 Milan, Italy

Synthesis and X-ray Structure of a Novel Technetium(IV) Complex with Tris(hydroxymethyl)(trimethylammonio)methane Iodide as a Ligand

R. Alberto,† A. Albinati,‡ G. Anderegg,*,† and G. Huber†

Received July 31, 1990

Until recently, the only known complexes of Tc(IV) with organic chelating ligands were dimers built around the characteristic "$[Tc(\mu\text{-}O)_2Tc]$" core.[1,2] As reported 5 years ago, mononuclear complexes have also been synthesized where the Tc(IV) center is coordinated to the oxygen atoms of an alcohol.[3] Examples of novel complexes of this type are those with ligands such as methanolate, glycolate, and the tridentate 1,2,4-butanetriolate. Glycerol, on the other hand, for steric reasons, cannot coordinate with all three oxygen atoms to the same metal center.[4] A promising group of other tridentate chelating alcoholato ligands are the derivates of tris(hydroxymethyl)methane, with a "tripod" structure. It has been reported that these alcohols, schematically shown in Figure 1, form stable complexes with metal centers of A type, e.g. Fe(III);[5] thus the formation of Tc(IV) complexes could be expected.

We, therefore, decided to investigate the "tripod" coordination chemistry of technetium and here report the synthesis and the X-ray structure of a stable mononuclear 1:2 Tc(IV) complex with a derivative of tris(hydroxymethyl)methane with $R = N(CH_3)_3^+$, i.e. the cation $(H_3THMT)^+$ that gives the complex $[Tc(THMT)_2]$.

Results and Discussion

Among the different derivatives of tris(hydroxymethyl)methane, THMT was chosen as a ligand for Tc(IV) for its coordinating properties. Indeed, the cationic substituent $R = N(CH_3)_3^+$ strongly reduces the basicity constants, allowing ligand deprotonation, and thus the complex formation may take place at a lower pH value (reducing the tendency for hydrolysis of the central ion in aqueous solution). Furthermore, the bulky substituent forces the ligand into a conformation that favors the tridentate mode of binding. This assumption was confirmed by preliminary results of investigations with the involved derivatives (e.g., the formation of the complex TcL_2^{2-} when the ligand has $R = H$ occurs at a much lower rate than with the chosen ligand).

This complex can be prepared in methanol according to the reactions shown in the Scheme I. From the iodide salt of the ligand $(H_3THMT)^+$ (**3**), compound **4** can be obtained either via the hexamethanolato complex of Tc(IV) (**2**), already described,[3] or by direct reaction of hexabromotechnetate(IV) (**1**) with **3** and subsequent neutralization of the liberated protons. The 1:2 complex $[Tc(THMT)_2]$ crystallizes only in presence of an excess of the ligand (as an iodide) (**3**) in the form of the double salt **4**. The reaction of $[H_3THMT]^+$ salts with Tc(V) compounds such as $[TcOCl_4]^-$ or $[TcO(OCH_2CH_2O)_2]^-$ yields $[Tc(THMT)_2]$ (65%) contaminated with small quantities of polymeric compounds (1-2%) and TcO_4^- (33%). It seems that "Tc^VTHMT" complexes are very unstable and quickly disproportionate in organic solvents according to the reaction

$$3Tc(V) \rightarrow 2Tc(IV) + Tc(VII)$$

The obtained Tc(IV) complex shows in methanolic solutions two maxima in the UV region (λ_{max} 295 and 225 nm) instead of one as obtained for other alcoholato complexes at similar wavelengths (λ_{max} 267-274 nm). In the IR spectra the observed band

* To whom correspondence should be addressed.
† ETH-Zentrum.
‡ University of Milan.

0020-1669/91/1330-3568$02.50/0